NEOPLASIA
www.neoplasia.com

Volume 14 Number 5 May 2012 pp. 420–428 420

Activation of Multiple ERBB Family Receptors Mediates Glioblastoma Cancer Stem–like Cell Resistance to EGFR-Targeted Inhibition[1,2]

Paul A. Clark*, Mari Iida†, Daniel M. Treisman*, Haviryaji Kalluri*, Sathyapriya Ezhilan*, Michael Zorniak*, Deric L. Wheeler†,‡ and John S. Kuo*,†,‡

*Department of Neurological Surgery, School of Medicine and Public Health, University of Wisconsin, Madison, WI; †Department of Human Oncology, School of Medicine and Public Health, University of Wisconsin, Madison, WI; ‡Carbone Cancer Center, School of Medicine and Public Health, University of Wisconsin, Madison, WI

Abstract

Epidermal growth factor receptor (EGFR) signaling is strongly implicated in glioblastoma (GBM) tumorigenesis. However, molecular agents targeting EGFR have demonstrated minimal efficacy in clinical trials, suggesting the existence of GBM resistance mechanisms. GBM cells with stem-like properties (CSCs) are highly efficient at tumor initiation and exhibit therapeutic resistance. In this study, GBM CSC lines showed sphere-forming and tumor initiation capacity after EGF withdrawal from cell culture media, compared with normal neural stem cells that rapidly perished after EGF withdrawal. Compensatory activation of related ERBB family receptors (ERBB2 and ERBB3) was observed in GBM CSCs deprived of EGFR signal (EGF deprivation or cetuximab inhibition), suggesting an intrinsic GBM resistance mechanism for EGFR-targeted therapy. Dual inhibition of EGFR and ERBB2 with lapatinib significantly reduced GBM proliferation in colony formation assays compared to cetuximab-mediated EGFR-specific inhibition. Phosphorylation of downstream ERBB signaling components (AKT, ERK1/2) and GBM CSC proliferation were inhibited by lapatinib. Collectively, these findings show that GBM therapeutic resistance to EGFR inhibitors may be explained by compensatory activation of EGFR-related family members (ERBB2, ERBB3) enabling GBM CSC proliferation, and therefore simultaneous blockade of multiple ERBB family members may be required for more efficacious GBM therapy.

Neoplasia (2012) 14, 420–428

Abbreviations: GBM, glioblastoma multiforme; CSC, cancer stem–like cell; NSC, neural stem cell; GFAP, glial fibrillary acidic protein; EGF, epidermal growth factor; EGFR, epidermal growth factor receptor; ERBB2 and ERBB3, v-erb-b erythroblastic leukemia viral oncogene homologs 2 and 3; bFGF, basic fibroblast growth factor; MRI, magnetic resonance imaging; DAPI, 4′,6-diamidino-2-phenylindole; TKI, tyrosine kinase inhibitor; RTK, receptor tyrosine kinase

Address all correspondence to: John S. Kuo, MD, PhD, K3/803 Clinical Science Center, Mail Code 8660, 600 Highland Ave, Madison, WI 53792-8660. E-mail: j.kuo@neurosurgery.wisc.edu

[1]P.A.C. was partially supported by a National Institutes of Health (NIH) T32 postdoctoral fellowship to the University of Wisconsin Stem Cell Training Program (NIH 5T32AG027566). M.Z. was partially supported by a NIH T32 fellowship to the University of Wisconsin Neuroscience Training Program (NIH T32GM007507). Funding support was also provided by the UW Carbone Cancer Center (NIH P30 CA014529), and also in the form of a SPORE grant to JSK and DLW. This work was supported by the HEADRUSH Brain Tumor Research Professorship, the AANS-NREF Young Clinician Investigator Award, Loff Memorial Fund, and funding to JSK from the Department of Neurological Surgery, Graduate School, and Medical School at the University of Wisconsin. This project was supported, in part, by grant P30CA014520 from the National Cancer Institute, grant 1UL1RR025011 from the Clinical and Translational Science Award program of the National Center for Research Resources, and the NIH (D.L.W.).
[2]This article refers to supplementary materials, which are designated by Table W1 and Figures W1 to W4 and are available online at www.neoplasia.com.
Received 23 February 2012; Revised 16 April 2012; Accepted 18 April 2012

DOI 10.1596/neo.12432

Introduction

Patients diagnosed with the brain cancer, glioblastoma (GBM), have a poor median survival of 14 months despite aggressive surgery, radiation, and chemotherapy [1,2]. Aberrant receptor tyrosine kinase (RTK) signaling is found in approximately 88% of GBMs [3]. In particular, the epidermal growth factor receptor (EGFR) is amplified or mutated in approximately half of GBMs, with 20% of tumors expressing the constitutively active mutant EGFRvIII protein [3–5]. Enhanced EGFR signaling in GBM leads to increased proliferation, survival, and invasion of tumor cells via downstream AKT and ERK1/2 signaling [4,6–9] and may be critical for GBM tumorigenesis. Because abnormal EGFR signaling is implicated in GBM and many other cancers, EGFR-targeting agents such as small-molecule tyrosine kinase inhibitors (TKIs, such as gefitinib, erlotinib, and lapatinib) and monoclonal antibodies (such as cetuximab and pertuzumab) have been developed for potential clinical use [10–12]. Unfortunately, clinical trials using EGFR inhibitors demonstrated only modest improvements in a small percentage of GBM patients [13–16], suggesting that many GBMs have intrinsic or rapidly acquire resistance to EGFR inhibition.

The cancer stem cell (CSC) theory posits that a small subpopulation of self-renewing "stem-like" cancer cells drives tumor propagation and recurrence [17,18]. CSCs have been isolated from GBM through AC/CD133 expression [19,20] or by sphere culture in stem cell medium [21–24] and are highly efficient at initiating phenocopies of the human neoplasm as xenografts forming with injection of as few as 10^2 to 10^3 CSCs into brains of immunodeficient mice [24,25]; if the injected tumor cells are first depleted of CSCs, cancer rarely develops [19]. In addition, GBM CSCs demonstrate resistance to commonly used anticancer therapies such as radiation [20] and chemotherapy [26,27]. Therefore, the current hypothesis is that therapeutically resistant GBM CSCs contribute to the observed rapid GBM recurrence resulting in poor patient survival, and therefore, CSC elimination is critical for effective therapies.

We hypothesized that GBM CSCs are involved in resistance to EGFR-specific inhibition. Supporting this hypothesis, Kelly et al. [25] demonstrated CSC propagation in the absence of exogenous growth factors (EGF and basic fibroblast growth factor [bFGF]), suggesting that these RTK signaling pathways may not be critical for GBM CSCs. However, confounding data are reported by other groups, which show that EGFR signaling is required for GBM CSC proliferation [28,29] and that addition of EGFR-specific inhibitors significantly decreased the sphere-forming and growth potential of exogenous growth factor–independent GBM CSCs [25]. In this study, we established multiple independent GBM CSC lines in the absence of exogenous mitogens (EGF and bFGF) to uncover and analyze potential resistance mechanisms of GBM CSCs to anti-EGFR therapies. GBM CSCs continued to proliferate as spheres in the absence of exogenous EGF and bFGF and retained tumor-initiating capability. We discovered that downstream activation of AKT and ERK pathways was maintained in GBM CSCs grown without exogenous mitogens, through activation of other EGFR-related receptor family members including ERBB2/HER2/neu and ERBB3/HER3. Lapatinib-mediated multireceptor inhibition of EGFR and ERBB2 was significantly more effective at preventing GBM CSC proliferation in colony formation assays compared with cetuximab-targeted inhibition of EGFR alone. Lapatinib treatment decreased downstream AKT and ERK activation in multiple independently derived GBM CSC lines. These results show that monotherapy against EGFR probably failed clinically for GBM because a subset of GBM cells are able to activate downstream signaling through related ERBB family members (ERBB2, ERBB3). Therefore, targeting of multiple ERBB family members is needed to overcome such resistance mechanisms and potentially achieve better clinical outcomes.

Materials and Methods

Isolation of GBM CSCs

All studies involving human tissue were performed with approval from the University of Wisconsin – Madison institutional review board with informed consent obtained from patients. GBM CSCs were isolated following protocols previously reported [21,23,30,31], with a few modifications. Tumor tissue was collected directly from the operating room, weighed, coarsely minced with a scalpel blade, and subsequently chopped twice at 200 μm using a tissue chopper (Sorvall TC-2 Smith-Farquahar). Chopped tissue was directly plated in suspension at 10 mg/ml in growth medium (passage medium [PM]: 70% Dulbecco modified Eagle medium–high glucose, 30% Ham's F12, 1× B27 supplement, 5 μg/ml heparin, penicillin-streptomycin-amphotericin (PSA), and 20 ng/ml each of EGF and bFGF) [30]. Cultures were passaged approximately every 7 to 10 days by tissue chopping twice at 200 μm. For initial studies, we used three different GBM CSC cell lines: two from primary (22 and 33) and one from recurrent (12.1) GBM. For later studies, additional GBM CSC lines were isolated through sphere culture (44 CSC) or growth on laminin substrates (15 and 99 CSC) [32]. Photomicrographs were taken using a Nikon Eclipse TE-2000 microscope (Nikon Instruments, Melville, NY) running MetaMorph 7.2 software. In all studies, GBM CSCs were compared to normal neural stem cells (NSCs). Human cortex fetal NSCs were a kind gift from Dr Clive Svendsen and were maintained as previously described [30].

Immunofluorescent Staining

Primary and secondary antibodies were purchased commercially: βIII-tubulin (G712A; Promega, Madison, WI); human nuclei (HuNu, MAB1281; Chemicon, Temecula, CA), CD(AC)133 (130-090-422; Miltenyi Biotec, Auburn, CA); nestin (ab5968), glial fibrillary acidic protein (GFAP; ab7779), and EGFR (ab52894) (all from Abcam, Cambridge, MA); and goat anti-IgG secondary antibodies Alexa Fluor 488 and 568 (Invitrogen, Grand Island, NY).

Medium-sized GBM CSC spheres (≈200-300 μm diameter) were seeded into eight-well chamber slides and incubated at 37°C for either 3 hours to test for stem cell markers and EGFR expression or 7 days in growth factor–depleted medium (minus EGF and bFGF) to test for glial (GFAP) and neuronal (βIII-tubulin) lineages. After incubation, cells were immediately fixed in 4% paraformaldehyde, blocked/permeabilized in 10% goat serum + 0.5% bovine serum albumin + 0.4% Triton X-100, and stained for 1 hour at room temperature with the following primary antibodies: anti–human nuclei (1:100), nestin (1:250), βIII-tubulin (1:2000), GFAP (1:1000), or EGFR (1:250). Fluorescent secondary antibodies (Alexa Fluor 488 or 568, 1:200) were then added for 1 hour at room temperature. Slides were then mounted with Prolong Gold with 4′,6-diamidino-2-phenylindole (DAPI; nuclear stain; Invitrogen). Fluorescent images were collected using epifluorescence (Nikon Eclipse TE-2000 microscope running MetaMorph 7.2 software) using appropriate filters. Normal NSCs were used as controls for all staining, and staining without primary antibody was performed as a control for nonspecific binding.

Flow Cytometry of Live Cells for Membrane Proteins

Antibodies EGFR (ab82194; Abcam) and CD(AC)133 preconjugated to R-PE (phycoerythrin) (130-080-801; Miltenyi Biotec) were used for flow cytometry. Secondary goat anti-IgG antibodies labeled with R-PE were purchased from Invitrogen.

GBM CSCs were dissociated with an enzyme-free cell dissociation buffer (Invitrogen), and approximately 10^6 cells were resuspended in flow cytometry buffer (PBS + 1% goat serum). For preconjugated CD133-R-PE (1:11), cells were incubated on ice for 1 hour and rinsed. For anti-EGFR antibody (1:50), cells were first incubated on ice for 1 hour with primary antibodies before rinsing and 1 hour of incubation on ice with species-specific secondary antibodies conjugated to R-PE (1:50). GBM CSCs were then analyzed using flow cytometry (FACScalibur; Becton Dickinson, Franklin Lakes, NJ). Isotype controls that received only secondary antibody to exclude nonspecific binding events and propidium iodide to determine live cells were used to gate data, which was analyzed using WinMDI freeware (http://facs.scripps.edu/software.html). A minimum of two independent experiments with duplicate samples (total $n = 4$) were performed; if results demonstrated high variability, a third independent experiment with duplicate samples was carried out.

Semiquantitative Reverse Transcription–Polymerase Chain Reaction for EGFRvIII Mutation

Presence of the EGFRvIII mutation in GBM CSCs was tested using reverse transcription–polymerase chain reaction (RT-PCR), using primers for EGFR/EGFRvIII as previously described [28]. Amplification conditions were 94°C for 2 minutes, followed by 42 cycles of denaturation at 95°C for 30 seconds, annealing at 56.5°C for 30 seconds, and extension at 68°C for 90 seconds. GAPDH functioned as housekeeping control with primers (forward, ACCACAGTCCATGCCATCAC; and reverse, TCCACCACCCTGTTGCTGTA); amplification conditions were 94°C for 2 minutes, followed by 24 cycles of denaturation at 95°C for 30 seconds, annealing at 57°C for 30 seconds, and extension at 68°C for 90 seconds.

GBM CSC Orthotopic Xenograft Model

Tumor initiation capacity of GBM CSCs under various conditions was verified by orthotopic xenograft as previously described [19,21,22], under a protocol approved by the Institutional Animal Care and Use Committee at UW-Madison. Briefly, GBM CSCs were enzymatically dissociated to single cells, and varying cell numbers (10^2-10^6) were suspended in 5 μl of PBS. Using a Hamilton syringe, the cells were stereotactically injected into the right striatum of anesthetized nonobese diabetic severe combined immunodeficient mice at 0.33 μl/min at the following coordinates referenced from bregma: 0 mm anteroposterior, +2.5 mm mediolateral, and −3.5 mm dorsoventral [22]. At either 3 months or onset of neurological symptoms, tumor formation was verified using magnetic resonance imaging (MRI). Mice were anesthetized, contrast enhanced using 10 mmol/kg of intraperitoneal gadodiamide [33] (Omniscan; GE Healthcare, Piscataway, NJ), and placed onto a small animal MRI scanner (4.7-T horizontal bore imaging/spectroscopy system; Varian , Palo Alto, CA), and T1- and T2-weighted images were obtained. As per animal protocol, once MRI showed tumor xenograft growth or when neurological symptoms were observed, injected nonobese diabetic severe combined immunodeficient mice were immediately euthanized by perfusion fixation with 4% paraformaldehyde, even if the animals were asymptomatic. Brains were then excised, embedded in paraffin, and processed for general histology.

Proliferation Assay

To test effects of exogenous mitogen withdrawal on short-term proliferation, 20,000 GBM CSCs were plated into 96 wells and allowed to proliferate for 4 days in respective medium +EGF/+bFGF or −EGF/−bFGF. Cell number was quantified using MTS assay, as per the manufacturer's instructions (CellTiter 96 AQueous Non-Radioactive Cell Proliferation Assay; Promega).

Colony-Forming Assay

Cetuximab was purchased from Bristol-Myers Squibb (Princeton, NJ). Lapatinib, gefitinib, and erlotinib were purchased from LC Laboratories (Woburn, MA). Pertuzumab was kindly provided by Genentech (San Francisco, CA). Doses used for gefitinib, erlotinib, cetuximab, and pertuzumab were determined from the literature as 50% inhibiting concentrations for head and neck cell lines [34,35]. Lapatinib dose was chosen as reported as the 50% inhibiting concentration for glioma cell lines [36].

GBM CSCs were enzymatically dissociated to single cells and seeded at 2000 cells/well into six-well plates precoated with poly-L-lysine/laminin. After cell recovery overnight, medium was exchanged with drug-containing medium, and afterward, fresh media containing drug were added twice a week. When GBM CSC colonies (>50 cells) became visible (≈2-4 weeks), cells were fixed and stained with 0.5% crystal violet in methanol for 5 minutes and rinsed extensively with distilled water. Colonies were then manually counted, with drug-treated conditions normalized to vehicle controls.

Immunoblot Analysis

Immunoblot analysis was performed as previously described [34], with a few modifications. The following antibodies were used: EGFR (sc-03), ERBB2/HER2/neu (sc-284), pERBB2 (Y1248) (sc-12352R), and ERBB3/HER3 (sc-285) were from Santa Cruz Biotechnology (Santa Cruz, CA); pERBB3 (Y1197) (4561), AKT (4691), pAKT (S473) (4060), ERK1/2 (4696), and pERK1/2 (Thr202/Tyr204) (9106), and α-tubulin (3873) from Cell Signaling Technology (Beverly, MA); pEGFR (Y1068) (ab32430) from Abcam; HRP-conjugated goat–anti-rabbit IgG (32460) and goat–anti-mouse IgG (32430) were purchased from Thermo Scientific (Waltham, MA).

For immunoblot analysis studies, GBM CSCs with and without exogenous mitogens were lysed using cell extraction buffer (FNN0011; Invitrogen) containing protease inhibitor cocktail (P8340; Sigma-Aldrich, St Louis, MO). Protein was quantified using a fluorescent-based total protein assay (EZQ Protein Quantitation, R33200; Invitrogen). Proteins (10 μg) were resuspended in 2× reducing sample buffer (Novex, LC2676; Invitrogen), electrophoresed on 10% to 20% Tris-glycine gels (Invitrogen), transferred using a semidry transfer system (Biorad, Hercules, CA) to polyvinylidene difluoride membranes (Millipore, Billerica, MA), and probed with specific antibodies. Detection of immunocomplexes was accomplished using luminescence (SuperSignal West Femto Maximum Sensitivity Substrate; Thermo Scientific), as per the manufacturer's instructions. For drug-related biochemical tests, exogenous growth factors were removed overnight from GBM CSCs. Drugs were then added to medium 2 hours before stimulation with EGF for 30 minutes, and GBM CSCs were collected and immunoblotted as above.

Results

Isolation and Validation of GBM CSC Lines

Cancer stem–like cell lines were successfully isolated from multiple patient GBM specimens using standard procedures. After approximately

2 to 4 weeks, small spheres were observed in culture, which continued to propagate in suspension (Figure 1). In our laboratory, the GBM CSCs propagated faster by passaging using the chopping technique used for some normal human NSC cultures [30], compared to passaging through mechanical dissociation, and were passaged every 7 to 10 days. Four independent GBM CSC lines were isolated through sphere culture: three from newly diagnosed (22, 33, 44) and one from a first recurrence (12.1). Two additional lines (15 and 99) were isolated through culture on laminin substrate using identical media conditions [32], and GBM CSCs isolated by either method exhibit similar genetic and phenotypic behaviors [32,37]. The three GBM CSC lines 12.1, 22, and 33 were chosen for most experiments. All GBM CSC lines expressed stem cell markers (CD133, nestin), detected by immunocytochemistry (Figure 1), and after removal of the mitogenic factors EGF and bFGF and attachment to poly-L-lysine/laminin–coated dishes, the GBM CSC differentiated and expressed markers of both glial (GFAP) and neuronal (βIII-tubulin) lineages, demonstrating their multilineage potential (Figure 1). Flow cytometry independently confirmed the uniform enrichment of GBM CSCs with CD133 expression (Figure 1), an NSC marker used in other published GBM CSC studies [19,31]. Importantly, the GBM CSCs also efficiently initiated orthotopic xenograft tumors within 12 to 16 weeks after injection of 2×10^5 GBM CSCs, as visualized by MRI and histology (Figure 1). Injection of 10^2 to 10^3 GBM CSCs initiated tumors (Table W1). GBM CSC xenografts were observed to recapitulate parental GBM phenotypes of diffusely infiltrating tumor cells, vascular proliferation, and areas of necrosis, although not all features were present for each GBM CSC line derived xenograft (Figures 1 and W1). This is in contrast to tumor models derived from injection of standard laboratory glioma cell lines, which yield discrete xenografts only with a high number of injected cells (>10^6 cells) [21]. No tumor xenografts were found in mice injected with an equal number of normal human NSCs after 6 months.

GBM CSCs Express EGF Signaling Components

Although growth factors such as EGF and bFGF are required for continued expansion of normal NSCs, GBM CSCs may have aberrant signaling mechanisms that allow them to escape normal regulation by these factors, similar to that described by Kelly et al. [25]. Immunocytochemistry demonstrated abundant and widespread EGFR expression in both GBM CSCs and human fetal NSCs (Figure 2, *A* and *B*); immunocytochemical staining results were also verified using immunoblot analysis (Figure 2*C*). The percentage of GBM CSC cells expressing EGFR as well as EGFR expression intensity was determined using flow cytometry (Figure 2*E*). Interestingly, NSCs exhibited significantly higher (≈4 times more EGFR$^+$ cells and ≈2 times higher intensity) EGFR expression than GBM CSCs did (Figure 2*F*; $P < .05$). The expression of the constitutively active, mutant EGFRvIII was not observed in GBM CSCs or in NSCs using semiquantitative RT-PCR (Figure 2*D*) [28].

GBM CSCs Are Maintained after Exogenous EGF Removal and Activate ERBB Family Signaling

We next determined the exogenous EGF requirement for GBM CSCs and possible compensation mechanisms in the absence of EGFR activation. For all tested GBM CSC lines as well as control NSCs, proliferation after 4 days was significantly reduced after removal of exogenous mitogens (Figure 3*A*; $P < .05$). However, NSCs exhibited a much greater reduction compared to the GBM CSC lines (NSC: +EGF/+bFGF = 100% ± 4.4%, −EGF/−bFGF = 29% ± 11%; 12.1: +EGF/+bFGF = 100% ± 11%, −EGF/−bFGF = 73% ± 11%; 22: +EGF/+bFGF = 100% ± 6.5%, −EGF/−bFGF = 79% ± 11%; 33: +EGF/+bFGF = 100% ± 7.4%, −EGF/−bFGF = 73% ± 6.5%; −EGF/−bFGF values normalized to +EGF/+bFGF values), and small spheres were only observed in GBM CSCs in −EGF/−bFGF conditions. In long-term culture, all GBM CSC lines continued to proliferate as spheres after exogenous mitogen removal (Figure 3*B*), although at a slower observed rate. Normal NSCs cultured under similar conditions failed to propagate. After adaptation for a minimum of 2 months with normal expansion and passaging, GBM CSC lines grown without exogenous mitogens were analyzed for stem cell, multilineage, and tumor-initiating properties. GBM CSCs without exogenous mitogens maintained expression of the stem cell marker nestin

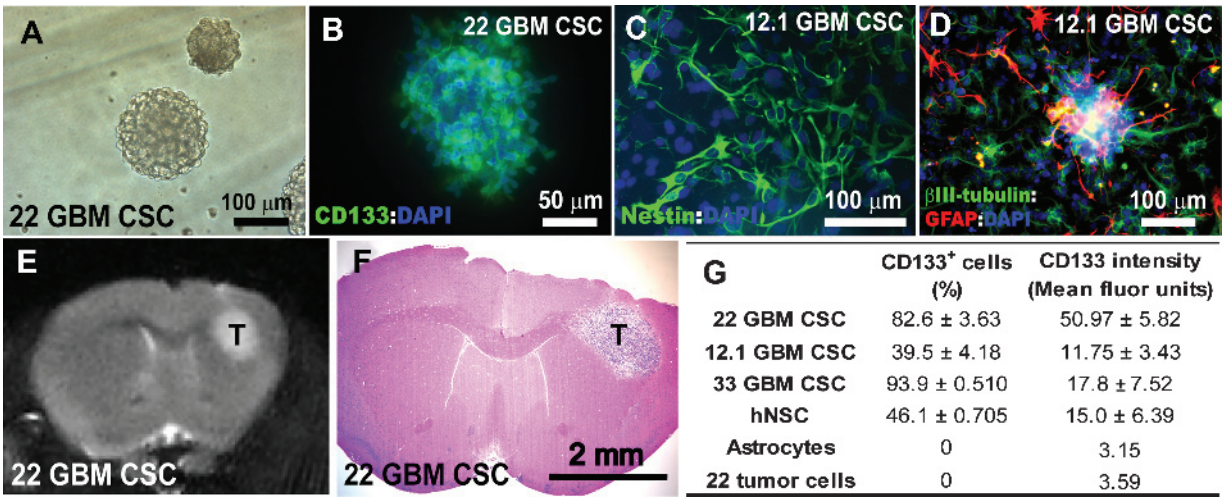

G	CD133$^+$ cells (%)	CD133 intensity (Mean fluor units)
22 GBM CSC	82.6 ± 3.63	50.97 ± 5.82
12.1 GBM CSC	39.5 ± 4.18	11.75 ± 3.43
33 GBM CSC	93.9 ± 0.510	17.8 ± 7.52
hNSC	46.1 ± 0.705	15.0 ± 6.39
Astrocytes	0	3.15
22 tumor cells	0	3.59

Figure 1. Characterization of GBM CSCs. Sphere-forming GBM CSCs from surgical specimens were obtained after 2 to 4 weeks of culture in stem cell medium (A) that expressed NSC markers (B: CD133, green; DAPI nuclear counterstain, blue; C: nestin, green) and demonstrated multilineage potential (D: βIII-tubulin/Tuj1, green; GFAP, red). Enrichment for CD133 was verified using flow cytometry (G). GBM CSCs initiated tumors 12 to 16 weeks after orthotopic injection, as evidenced by MRI (E: 22 GBM CSCs, 100,000 cells, 106 days after injection; T1-weighted with gadolinium enhancement) and histology (F: hematoxylin and eosin). T indicates tumor.

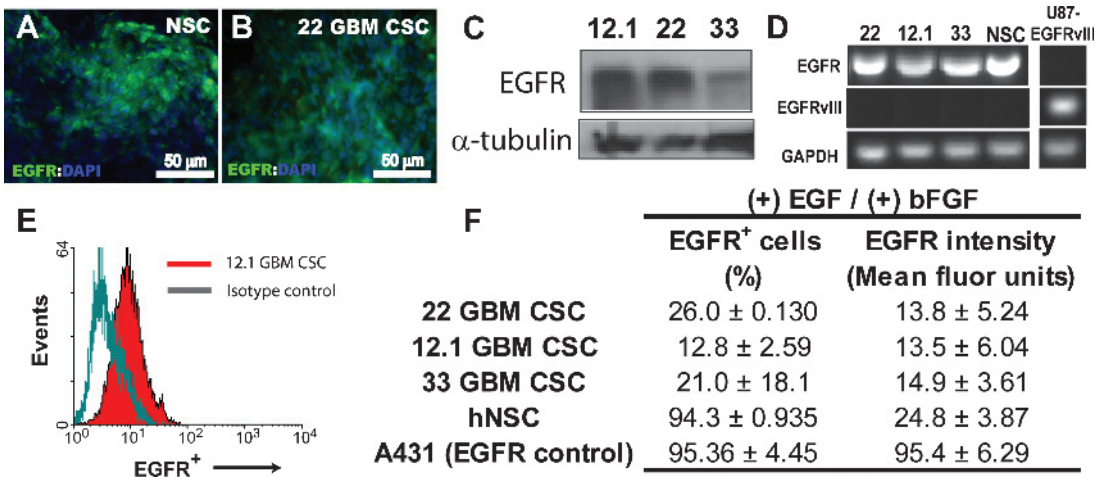

F

	(+) EGF / (+) bFGF	
	EGFR$^+$ cells (%)	EGFR intensity (Mean fluor units)
22 GBM CSC	26.0 ± 0.130	13.8 ± 5.24
12.1 GBM CSC	12.8 ± 2.59	13.5 ± 6.04
33 GBM CSC	21.0 ± 18.1	14.9 ± 3.61
hNSC	94.3 ± 0.935	24.8 ± 3.87
A431 (EGFR control)	95.36 ± 4.45	95.4 ± 6.29

Figure 2. EGFR signaling components are present in GBM CSCs. Immunocytochemistry demonstrated expression of EGFR on both NSCs (A) and GBM CSCs (B). EGFR expression was validated for all GBM CSC lines using Western immunoblot analysis (C), semiquantitative PCR (D), and flow cytometry (E and F). Flow cytometry analysis showed presence of EGFR expression in all GBM CSC lines, although at varying levels, and NSCs demonstrated a significantly higher percentage of EGFR$^+$ cells compared to GBM CSCs (F). Presence of the common EGFRvIII mutation was tested using semiquantitative RT-PCR and was not present in any of the isolated GBM CSC lines (D).

(Figure 3*C*), multilineage potential (Figure 3*D*), and tumor-initiating capacity in immunodeficient mice (Figures 3*E* and W1). Sphere-forming GBM CSCs were also recovered from xenografts that exhibited stem cell marker expression and multilineage potential (data not shown). Flow cytometric analysis of GBM CSCs cultured long-term without exogenous mitogens demonstrated significantly decreased CD133$^+$ cells and CD133 expression and increased EGFR$^+$ cells and EGFR expression (Figures 3*G* and W2; $P < .05$ compared to standard growth conditions).

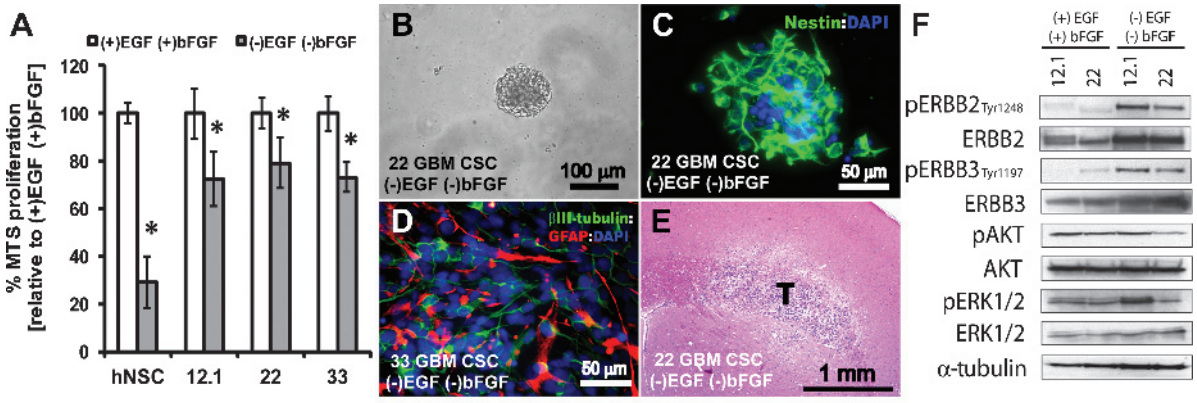

G

	Standard Growth Conditions (+ EGF, + bFGF)		Mitogens Removed (- EGF, - bFGF)		Mitogen Re-addition (+ EGF, + bFGF)	
	CD133$^+$ cells (%)	CD133 intensity (Mean fluor units)	CD133$^+$ cells (%)	CD133 intensity (Mean fluor units)	CD133$^+$ cells (%)	CD133 intensity (Mean fluor units)
22 GBM CSC	82.6 ± 3.63	50.97 ± 5.82	0.77 ± 0.98 *	6.2 ± 1.33	2.56 ± 1.39	4.7 ± 1.17
12.1 GBM CSC	39.5 ± 4.18	11.75 ± 3.43	6.23 ± 3.47 *	8.09 ± 0.47	0.615 ± 0.105	3.70 ± 1.15
33 GBM CSC	93.9 ± 0.510	17.8 ± 7.52	8.91 ± 2.99 *	6.39 ± 1.3	21.3 ± 4.86	10.9 ± 0.965
	EGFR$^+$ cells (%)	EGFR intensity (Mean fluor units)	EGFR$^+$ cells (%)	EGFR intensity (Mean fluor units)	EGFR$^+$ cells (%)	EGFR intensity (Mean fluor units)
22 GBM CSC	26.0 ± 0.130	13.8 ± 5.24	57.1 ± 6.04 *	36.81 ± 1.30	0.35 ± 0.165	4.38 ± 0.04
12.1 GBM CSC	12.8 ± 2.59	13.5 ± 6.04	78.3 ± 6.80 *	35.15 ± 3.99	3.80 ± 3.94	6.48 ± 0.31
33 GBM CSC	21.0 ± 18.1	14.9 ± 3.61	94.8 ± 1.52 *	95.8 ± 1.52	3.52 ± 0.625	6.21 ± 0.240

Figure 3. GBM CSCs propagate independent of exogenous EGF with increased activation of ERBB family receptors. Removal of exogenous EGF and bFGF significantly reduced short-term (4 days) proliferation of NSCs and GBM CSCs (*$P < .05$), although the antiproliferative effect was less in the GBM CSC lines compared to NSCs (A). Unlike NSCs that growth arrested without addition of exogenous EGF and bFGF, GBM CSCs continued to propagate *in vitro* as spheres (B). GBM CSCs without exogenous mitogens maintained expression of the stem cell marker nestin (C: green; DAPI nuclear counterstain, blue), multilineage potential (D: βIII-tubulin/Tuj1, green; GFAP, red), and tumor initiation capacity (E: 22 GBM CSC −EGF/−bFGF, 100,000 cells, 90 days). Flow cytometry analysis of GBM CSC −EGF/−bFGF demonstrated significantly decreased CD133 expression and increased EGFR expression (G: *$P < .05$). CD133 expression did not return on mitogen readdition and subculture, whereas EGFR expression decreased (G). Immunoblot analysis demonstrated increased ERBB family activation (ERBB2, ERBB3) and maintained downstream pAKT and pERK1/2 in GBM CSCs without EGF and bFGF compared to +EGF/+bFGF (F).

$CD133^+$ cells and CD133 expression did not recover for the GBM CSCs after exogenous mitogen readdition and subculture, whereas $EGFR^+$ cells and EGFR expression was reduced (Figures 3*G* and W2). Altogether, self-renewing multipotent GBM CSCs that were able to initiate tumors survived and propagated after withdrawal of exogenous mitogens.

We used immunoblot analysis to analyze signaling within the GBM CSCs (12.1 and 22) with and without exogenous EGF and bFGF in an attempt to uncover mechanisms that allow continued growth of the cells without exogenous mitogenic stimulation. Conceptually, these mechanisms may represent inherent GBM CSC resistance to anti-EGFR therapies. Not surprisingly, downstream activation of AKT and ERK1/2 (MAPK) remained relatively constant with GBM CSC culture with and without exogenous EGF (Figure 3*E*). Multiple reports have identified these downstream pathways as critical in GBM and CSC survival and propagation [14,16,28,29,38]. Up-regulation and activation of the ERBB family receptors ERBB2 and ERBB3 were also observed after exogenous mitogen removal from GBM CSCs (Figure 3*E*), thereby suggesting that compensatory ERBB2/3 activation maintained downstream AKT and MAPK signaling in CSCs.

ERBB Family Signaling Is Required for GBM CSC Proliferation

To test the contribution of ERBB2 to GBM CSC proliferation after removal of exogenous EGF and bFGF, GBM CSC colony formation assays after addition of the dual TKI lapatinib (blocks activation of both EGFR and ERBB2) [39] were compared with cetuximab blockade of EGFR alone. This experiment also addresses the possibility of endogenous or autologous EGFR activation. Before colony formation assays, immunoblot analysis was used to verify robust blockade of EGFR activation using cetuximab (100 nM) and lapatinib (5 μM) in GBM CSC lines (12.1 and 22 GBM CSCs +EGF/+bFGF; Figure W3). We also verified that multiple monospecific EGFR inhibitors encompassing blocking antibodies as well as TKIs failed to decrease downstream EGFR signaling (Figure W4). Addition of cetuximab (100 nM) [34,35] to GBM CSCs with exogenous mitogens significantly reduced their colony-forming ability compared to vehicle controls (68% ± 3.9% of control for 22 CSC and 49% ± 3.2% for 12.1 CSC, $P < .05$; Figure 4). In GBM CSCs cultured without exogenous EGF and bFGF, cetuximab's effect was greatly attenuated (89% ± 2.9% of control for 22 CSC and 89% ± 1.3% for 12.1 CSC, $P < .05$). Lapatinib (5 μM) [36,40,41] strongly inhibited colony formation by GBM CSCs cultured in media with or without exogenous EGF and bFGF (27% ± 2.7% of control for 22 CSC and 13% ± 2.0% of control for 22 CSC –EGF; 9.7% ± 2.8% for 12.1 CSC and 16% ± 4.8% for 12.1 CSC(–)EGF; $P < .05$; Figure 4). Lapatinib also successfully reduced downstream pAKT and pERK1/2 signaling in 12.1 and 22 GBM CSCs shown by immunoblot analysis (Figure 4*D*). The effects of EGFR and ERBB2 inhibition were also tested in four additional GBM CSC lines cultured in the presence of EGF and bFGF. Cetuximab inhibited growth of all GBM CSC lines (15, 33, 44, and 99) tested, decreasing colony formation from 19% to 43% compared to vehicle controls ($P < .05$). However, dual targeting of EGFR and ERBB2 using lapatinib was significantly more effective at inhibiting proliferation compared to cetuximab (67%-87% total reduction, $P < .05$). Immunoblot analysis demonstrated a range of pAKT and pERK1/2 inhibition in these additional GBM CSC lines.

Discussion

Growth factor–stimulated RTK signaling, particularly aberrant EGF receptor activation, is gaining much attention in both cancer and CSC biology. Multiple TKIs and blocking monoclonal antibodies

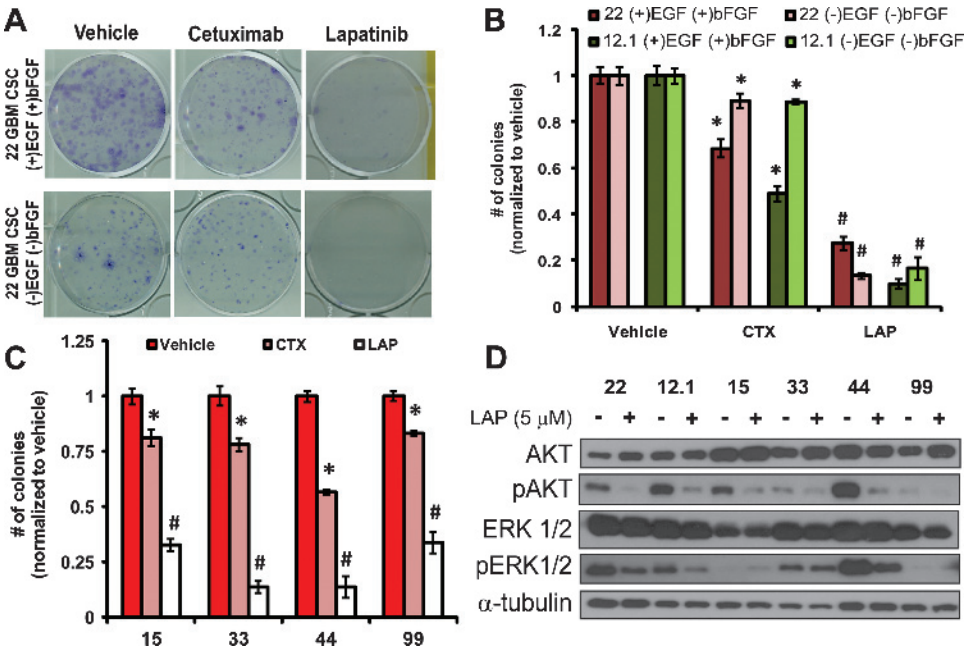

Figure 4. Dual blockade of EGFR and ERBB2 prevents propagation of GBM CSCs. Cetuximab (inhibitory EGFR antibody, 100 nM) inhibited colony-forming ability of GBM CSCs, but the effect is heavily attenuated in GBM CSCs without exogenous EGF and bFGF (A, B) (*$P < .05$). Lapatinib (EGFR/ERBB2 TKI, 5 μM) inhibited colony formation by GBM CSCs from either growth condition equally (A, B). Lapatinib also significantly better prevented colony formation in an additional four GBM CSC lines, compared to cetuximab (C). Immunoblot analysis demonstrated reduced AKT activation with lapatinib after EGF stimulation, as well as reduced pERK1/2 in three of the GBM CSC lines (22, 12.1, and 44) (D).

are already in clinical use for various cancers such as lung, head/neck, breast, colorectal, and others [10–12,42], with many second-generation EGFR inhibitors also in clinical trials [43,44]. In brain tumors, EGFR is overexpressed in up to 50% of GBMs [45] with the EGFR variant III (EGFRvIII) mutation (confers constitutive EGF signaling) present in up to 40% of EGFR-amplified GBMs [5,46]. Despite the seemingly critical role of EGFR signaling in GBM, initial clinical trials have only shown modest improvements in a small percentage of patients [13–16]. These initial clinical results demonstrate the importance of understanding GBM resistance mechanisms to EGFR and other molecular inhibitors toward developing more effective treatments.

Within GBM, the CSC subpopulation likely harbors intrinsic or rapidly acquired resistance to EGFR inhibitors as for other chemotherapeutics [26,27,47]. In this study, we removed exogenous mitogens present in GBM CSC culture medium as a means of investigating GBM CSC responses to disruption of EGFR signaling. We identified activation of compensatory ERBB family members, specifically ERBB2 and ERBB3, in GBM CSCs deprived of exogenous EGF, suggesting blockade of multiple ERBB family members is required for successful GBM CSC eradication. This was shown through addition of lapatinib, a dual TKI directed at EGFR and ERBB2, to effectively prevent GBM CSC colony formation in all tested independent GBM CSC lines.

These results of EGFR blockade within GBM CSCs are in line with and extend recently reported results [25,28,29]. Soeda et al. [28] tested multiple growth factors for their ability to promote sphere formation in three independent brain tumor lines and found that EGF stimulation was required for sphere formation. In contrast, Kelly et al. [25] successfully generated CSC cultures from 8 of 11 GBM samples in the absence of exogenous mitogens (–EGF/–bFGF). Although timing of the studies was different, as Soeda et al. [28] tested sphere formation after 7 days and Kelly et al. [25] established ongoing cultures directly from patient specimens, these studies suggest variable GBM CSC growth factor requirements between samples. Our results for three established GBM CSC lines correlates with the findings of Kelly et al. [25]; when cultured without exogenous mitogens (EGF and bFGF), GBM CSCs continued to self-renew and maintained multipotency and tumor initiation capability. The comparison controls of normal NSCs did not form spheres or survive without exogenous growth factors, in agreement with Kelly et al. [25], so growth factor–free survival seems to be a CSC oncogenic property. In this study, we demonstrate that continued GBM CSC propagation after EGF removal is at least partially due to activation of ERBB family signaling. Our data along with the reported studies suggest that EGFR signaling is required for GBM CSC propagation, but the CSCs can rapidly activate related RTKs to maintain downstream signaling pathways for survival.

Although not investigated in this study, it will be important to determine the drivers of the compensatory ERBB signaling found in GBM CSCs after EGF deprivation. Genetically, the constitutively active EGFRvIII mutation was not identified in any of the GBM CSC lines (Figure 2), and we have additionally demonstrated that the main EGFR kinase domain abnormalities found in lung cancer are not present in the tested GBM CSC lines (data not shown). Autocrine or paracrine stimulation of EGFR through ligands such as EGF or amphiregulin, among others, may also confer survival and proliferative cues to GBM CSCs independent of exogenous EGF. These types of signaling may explain the small but significant effect of cetuximab at inhibiting GBM CSC colony formation in medium without exogenous mitogens (Figure 4); however, lapatinib treatment resulted in greater inhibition of colony formation, suggesting that autocrine or paracrine EGFR stimulation is only partially responsible for GBM CSC exogenous mitogen independence. Finally, multiple reports have now identified neuregulin ligands as potential drivers in ERBB-dependent cancers such as head and neck, colon, and lung [42,48]. Neuregulin ligands activate ERBB family members ERBB3 or ERBB4 that dimerize with other family members as well as activating their own downstream signaling [49,50], and future work will need to determine the role of neuregulins in GBM CSC growth and resistance to EGFR inhibitors.

The role of ERBB family signaling in resistance to molecular inhibitors is rapidly becoming appreciated in many forms of cancer [34,42,51–53]. In glioma, the role of ERBB2 and ERBB3 signaling in progression and resistance remains largely unknown. Some GBM cell lines express ERBB2, including A172 and U251MG, and have been shown to be sensitive either to ERBB2-inhibiting antibodies or lapatinib [36,54]. Detection of ERBB2 in GBM and grade 3 gliomas has also been reported, with low-ERBB2 expression correlated with a better prognosis [55]. Early clinical trials have demonstrated reduced pEGFR and pAKT after 7 days of lapatinib treatment in six of nine patients tested; however, completion of the trial with reported survival is still forthcoming [38].

Lastly, a caveat of the current study relates to lapatinib dosing. In addition to specific EGFR- and ERBB2-targeted inhibition, other "off-target" lapatinib activities have been reported—including inhibition of glutathione *S*-transferase P1 (GSTP1) [41], inhibition of nuclear translocation of EGFR and ERBB2 [56], and inhibition of sterol regulatory element-binding protein-1 (SREBP-1) to block fatty acid synthesis [38]. Future studies will investigate the contribution (if any) of these "nonspecific" lapatinib effects in targeting GBM CSC proliferation.

In summary, this study provides an explanation for previous confounding reports showing the importance and necessity of aberrant EGFR activation in GBMs, yet failure of EGFR-targeted inhibition therapy in GBM clinical trials. We show that a subset of GBM cells, the GBM CSCs, exhibit therapeutic resistance and proliferate despite EGF deprivation or cetuximab-mediated EGFR inhibition through compensatory activation of EGFR-related family members (ERBB2, ERBB3). Importantly, only GBM CSCs proliferate, whereas normal NSCs did not survive in the absence of EGFR signaling, implicating ERBB2 and ERBB3 compensation in GBM CSCs as a tumorigenic mechanism. The presence of this resistance mechanism in GBM CSCs, which is able to recapitulate GBM, likely contributes to the clinically observed rapid tumor recurrence and suggests that it is worthwhile to explore multi-EGFR receptor family inhibition as a component of more effective GBM treatment strategies.

Acknowledgments

The authors thank the gifts of human NSCs from Dr Clive Svendsen (Cedars-Sinai Regenerative Medicine Center, Los Angeles, CA) and his expert advice. The authors also thank Frank Hospod for expert technical assistance.

References

[1] Stupp R, Mason WP, van den Bent MJ, Weller M, Fisher B, Taphoorn MJ, Belanger K, Brandes AA, Marosi C, Bogdahn U, et al. (2005). Radiotherapy plus concomitant and adjuvant temozolomide for glioblastoma. *N Engl J Med* **352**, 987–996.

[2] Lacroix M, Abi-Said D, Fourney DR, Gokaslan ZL, Shi W, DeMonte F, Lang FF, McCutcheon IE, Hassenbusch SJ, Holland E, et al. (2001). A multivariate analysis of 416 patients with glioblastoma multiforme: prognosis, extent of resection, and survival. *J Neurosurg* **95**, 190–198.

[3] TCGA (2008). Comprehensive genomic characterization defines human glioblastoma genes and core pathways. *Nature* **455**, 1061–1068.
[4] Lassman AB (2004). Molecular biology of gliomas. *Curr Neurol Neurosci Rep* **4**, 228–233.
[5] Aldape KD, Ballman K, Furth A, Buckner JC, Giannini C, Burger PC, Scheithauer BW, Jenkins RB, and James CD (2004). Immunohistochemical detection of EGFRvIII in high malignancy grade astrocytomas and evaluation of prognostic significance. *J Neuropathol Exp Neurol* **63**, 700–707.
[6] Molina JR, Hayashi Y, Stephens C, and Georgescu MM (2010). Invasive glioblastoma cells acquire stemness and increased Akt activation. *Neoplasia* **12**, 453–463.
[7] Blume-Jensen P and Hunter T (2001). Oncogenic kinase signalling. *Nature* **411**, 355–365.
[8] Hambardzumyan D, Becher OJ, Rosenblum MK, Pandolfi PP, Manova-Todorova K, and Holland EC (2008). PI3K pathway regulates survival of cancer stem cells residing in the perivascular niche following radiation in medulloblastoma *in vivo*. *Genes Dev* **22**, 436–448.
[9] Ayuso-Sacido A, Moliterno JA, Kratovac S, Kapoor GS, O'Rourke DM, Holland EC, Garcia-Verdugo JM, Roy NS, and Boockvar JA (2009). Activated EGFR signaling increases proliferation, survival, and migration and blocks neuronal differentiation in post-natal neural stem cells. *J Neurooncol* **97**, 323–337.
[10] Gupta A and Raina V (2010). Geftinib. *J Cancer Res Ther* **6**, 249–254.
[11] Harari PM, Allen GW, and Bonner JA (2007). Biology of interactions: anti-epidermal growth factor receptor agents. *J Clin Oncol* **25**, 4057–4065.
[12] Vivanco I and Mellinghoff IK (2010). Epidermal growth factor receptor inhibitors in oncology. *Curr Opin Oncol* **22**, 573–578.
[13] Lassman AB, Rossi MR, Raizer JJ, Abrey LE, Lieberman FS, Grefe CN, Lamborn K, Pao W, Shih AH, Kuhn JG, et al. (2005). Molecular study of malignant gliomas treated with epidermal growth factor receptor inhibitors: tissue analysis from North American Brain Tumor Consortium Trials 01-03 and 00-01. *Clin Cancer Res* **11**, 7841–7850.
[14] Mellinghoff IK, Wang MY, Vivanco I, Haas-Kogan DA, Zhu S, Dia EQ, Lu KV, Yoshimoto K, Huang JH, Chute DJ, et al. (2005). Molecular determinants of the response of glioblastomas to EGFR kinase inhibitors. *N Engl J Med* **353**, 2012–2024.
[15] Peereboom DM, Shepard DR, Ahluwalia MS, Brewer CJ, Agarwal N, Stevens GH, Suh JH, Toms SA, Vogelbaum MA, Weil RJ, et al. (2010). Phase II trial of erlotinib with temozolomide and radiation in patients with newly diagnosed glioblastoma multiforme. *J Neurooncol* **98**, 93–99.
[16] Raizer JJ, Abrey LE, Lassman AB, Chang SM, Lamborn KR, Kuhn JG, Yung WK, Gilbert MR, Aldape KA, Wen PY, et al. (2010). A phase II trial of erlotinib in patients with recurrent malignant gliomas and nonprogressive glioblastoma multiforme postradiation therapy. *Neuro Oncol* **12**, 95–103.
[17] Bonnet D and Dick JE (1997). Human acute myeloid leukemia is organized as a hierarchy that originates from a primitive hematopoietic cell. *Nat Med* **3**, 730–737.
[18] Clarke MF, Dick JE, Dirks PB, Eaves CJ, Jamieson CH, Jones DL, Visvader J, Weissman IL, and Wahl GM (2006). Cancer stem cells—perspectives on current status and future directions: AACR Workshop on Cancer Stem Cells. *Cancer Res* **66**, 9339–9344.
[19] Singh SK, Hawkins C, Clarke ID, Squire JA, Bayani J, Hide T, Henkelman RM, Cusimano MD, and Dirks PB (2004). Identification of human brain tumour initiating cells. *Nature* **432**, 396–401.
[20] Bao S, Wu Q, McLendon RE, Hao Y, Shi Q, Hjelmeland AB, Dewhirst MW, Bigner DD, and Rich JN (2006). Glioma stem cells promote radioresistance by preferential activation of the DNA damage response. *Nature* **444**, 756–760.
[21] Lee J, Kotliarova S, Kotliarov Y, Li A, Su Q, Donin NM, Pastorino S, Purow BW, Christopher N, Zhang W, et al. (2006). Tumor stem cells derived from glioblastomas cultured in bFGF and EGF more closely mirror the phenotype and genotype of primary tumors than do serum-cultured cell lines. *Cancer Cell* **9**, 391–403.
[22] Galli R, Binda E, Orfanelli U, Cipelletti B, Gritti A, De Vitis S, Fiocco R, Foroni C, Dimeco F, and Vescovi A (2004). Isolation and characterization of tumorigenic, stem-like neural precursors from human glioblastoma. *Cancer Res* **64**, 7011–7021.
[23] Ignatova TN, Kukekov VG, Laywell ED, Suslov ON, Vrionis FD, and Steindler DA (2002). Human cortical glial tumors contain neural stem–like cells expressing astroglial and neuronal markers *in vitro*. *Glia* **39**, 193–206.
[24] Wakimoto H, Mohapatra G, Kanai R, Curry WT Jr, Yip S, Nitta M, Patel AP, Barnard ZR, Stemmer-Rachamimov AO, Louis DN, et al. (2012). Maintenance of primary tumor phenotype and genotype in glioblastoma stem cells. *Neuro Oncol* **14**, 132–144.
[25] Kelly JJ, Stechishin O, Chojnacki A, Lun X, Sun B, Senger DL, Forsyth P, Auer RN, Dunn JF, Cairncross JG, et al. (2009). Proliferation of human glioblastoma stem cells occurs independently of exogenous mitogens. *Stem Cells* **27**, 1722–1733.
[26] Bleau AM, Hambardzumyan D, Ozawa T, Fomchenko EI, Huse JT, Brennan CW, and Holland EC (2009). PTEN/PI3K/Akt pathway regulates the side population phenotype and ABCG2 activity in glioma tumor stem–like cells. *Cell Stem Cell* **4**, 226–235.
[27] Liu G, Yuan X, Zeng Z, Tunici P, Ng H, Abdulkadir IR, Lu L, Irvin D, Black KL, and Yu JS (2006). Analysis of gene expression and chemoresistance of $CD133^+$ cancer stem cells in glioblastoma. *Mol Cancer* **5**, 67.
[28] Soeda A, Inagaki A, Oka N, Ikegame Y, Aoki H, Yoshimura S, Nakashima S, Kunisada T, and Iwama T (2008). Epidermal growth factor plays a crucial role in mitogenic regulation of human brain tumor stem cells. *J Biol Chem* **283**, 10958–10966.
[29] Griffero F, Daga A, Marubbi D, Capra MC, Melotti A, Pattarozzi A, Gatti M, Bajetto A, Porcile C, Barbieri F, et al. (2009). Different response of human glioma tumor–initiating cells to epidermal growth factor receptor kinase inhibitors. *J Biol Chem* **284**, 7138–7148.
[30] Svendsen CN, ter Borg MG, Armstrong RJ, Rosser AE, Chandran S, Ostenfeld T, and Caldwell MA (1998). A new method for the rapid and long term growth of human neural precursor cells. *J Neurosci Methods* **85**, 141–152.
[31] Singh SK, Clarke ID, Terasaki M, Bonn VE, Hawkins C, Squire J, and Dirks PB (2003). Identification of a cancer stem cell in human brain tumors. *Cancer Res* **63**, 5821–5828.
[32] Pollard SM, Yoshikawa K, Clarke ID, Danovi D, Stricker S, Russell R, Bayani J, Head R, Lee M, Bernstein M, et al. (2009). Glioma stem cell lines expanded in adherent culture have tumor-specific phenotypes and are suitable for chemical and genetic screens. *Cell Stem Cell* **4**, 568–580.
[33] Bourasset F, Dencausse A, Bourrinet P, Ducret M, and Corot C (2001). Comparison of plasma and peritoneal concentrations of various categories of MRI blood pool agents in a murine experimental pharmacokinetic model. *Magma* **12**, 82–87.
[34] Wheeler DL, Huang S, Kruser TJ, Nechrebecki MM, Armstrong EA, Benavente S, Gondi V, Hsu KT, and Harari PM (2008). Mechanisms of acquired resistance to cetuximab: role of HER (ErbB) family members. *Oncogene* **27**, 3944–3956.
[35] Wheeler DL, Iida M, Kruser TJ, Nechrebecki MM, Dunn EF, Armstrong EA, Huang S, and Harari PM (2009). Epidermal growth factor receptor cooperates with Src family kinases in acquired resistance to cetuximab. *Cancer Biol Ther* **8**, 696–703.
[36] Giannopoulou E, Dimitropoulos K, Argyriou AA, Koutras AK, Dimitrakopoulos F, and Kalofonos HP (2009). An *in vitro* study, evaluating the effect of sunitinib and/or lapatinib on two glioma cell lines. *Invest New Drugs* **28**, 554–560.
[37] Lottaz C, Beier D, Meyer K, Kumar P, Hermann A, Schwarz J, Junker M, Oefner PJ, Bogdahn U, and Wischhusen J, et al. (2010). Transcriptional profiles of $CD133^+$ and $CD133^-$ glioblastoma-derived cancer stem cell lines suggest different cells of origin. *Cancer Res* **70**, 2030–2040.
[38] Guo D, Prins RM, Dang J, Kuga D, Iwanami A, Soto H, Lin KY, Huang TT, Akhavan D, Hock MB, et al. (2009). EGFR signaling through an Akt-SREBP-1–dependent, rapamycin-resistant pathway sensitizes glioblastomas to antilipogenic therapy. *Sci Signal* **2**, ra82.
[39] Nelson MH and Dolder CR (2006). Lapatinib: a novel dual tyrosine kinase inhibitor with activity in solid tumors. *Ann Pharmacother* **40**, 261–269.
[40] Xia W, Husain I, Liu L, Bacus S, Saini S, Spohn J, Pry K, Westlund R, Stein SH, and Spector NL (2007). Lapatinib antitumor activity is not dependent upon phosphatase and tensin homologue deleted on chromosome 10 in ErbB2-overexpressing breast cancers. *Cancer Res* **67**, 1170–1175.
[41] Okamura T, Singh S, Buolamwini J, Haystead T, Friedman H, Bigner D, and Ali-Osman F (2009). Tyrosine phosphorylation of the human glutathione *S*-transferase P1 by epidermal growth factor receptor. *J Biol Chem* **284**, 16979–16989.
[42] Yonesaka K, Zejnullahu K, Okamoto I, Satoh T, Cappuzzo F, Souglakos J, Ercan D, Rogers A, Roncalli M, Takeda M, et al. (2011). Activation of ERBB2 signaling causes resistance to the EGFR-directed therapeutic antibody cetuximab. *Sci Transl Med* **3**, 99ra86.
[43] Mukherji D and Spicer J (2009). Second-generation epidermal growth factor tyrosine kinase inhibitors in non–small cell lung cancer. *Expert Opin Investig Drugs* **18**, 293–301.

[44] Machiels JP and Schmitz S (2011). Molecular-targeted therapy of head and neck squamous cell carcinoma: beyond cetuximab-based therapy. *Curr Opin Oncol* **23**, 241–248.

[45] Halatsch ME, Schmidt U, Behnke-Mursch J, Unterberg A, and Wirtz CR (2006). Epidermal growth factor receptor inhibition for the treatment of glioblastoma multiforme and other malignant brain tumours. *Cancer Treat Rev* **32**, 74–89.

[46] Collins VP and James CD (1993). Gene and chromosomal alterations associated with the development of human gliomas. *FASEB J* **7**, 926–930.

[47] Gong X, Schwartz PH, Linskey ME, and Bota DA (2011). Neural stem/progenitors and glioma stem–like cells have differential sensitivity to chemotherapy. *Neurology* **76**, 1126–1134.

[48] Wilson TR, Lee DY, Berry L, Shames DS, and Settleman J (2011). Neuregulin-1–mediated autocrine signaling underlies sensitivity to HER2 kinase inhibitors in a subset of human cancers. *Cancer Cell* **20**, 158–172.

[49] Yarden Y and Sliwkowski MX (2001). Untangling the ErbB signalling network. *Nat Rev Mol Cell Biol* **2**, 127–137.

[50] Montero JC, Rodriguez-Barrueco R, Ocana A, Diaz-Rodriguez E, Esparis-Ogando A, and Pandiella A (2008). Neuregulins and cancer. *Clin Cancer Res* **14**, 3237–3241.

[51] Baselga J and Swain SM (2009). Novel anticancer targets: revisiting ERBB2 and discovering ERBB3. *Nat Rev Cancer* **9**, 463–475.

[52] Quesnelle KM and Grandis JR (2011). Dual kinase inhibition of EGFR and HER2 overcomes resistance to cetuximab in a novel *in vivo* model of acquired cetuximab resistance. *Clin Cancer Res* **17**, 5935–5944.

[53] Ritter CA, Perez-Torres M, Rinehart C, Guix M, Dugger T, Engelman JA, and Arteaga CL (2007). Human breast cancer cells selected for resistance to trastuzumab *in vivo* overexpress epidermal growth factor receptor and ErbB ligands and remain dependent on the ErbB receptor network. *Clin Cancer Res* **13**, 4909–4919.

[54] Mineo JF, Bordron A, Quintin-Roue I, Loisel S, Ster KL, Buhe V, Lagarde N, and Berthou C (2004). Recombinant humanised anti-HER2/neu antibody (Herceptin) induces cellular death of glioblastomas. *Br J Cancer* **91**, 1195–1199.

[55] Mineo JF, Bordron A, Baroncini M, Maurage CA, Ramirez C, Siminski RM, Berthou C, and Dam Hieu P (2007). Low HER2-expressing glioblastomas are more often secondary to anaplastic transformation of low-grade glioma. *J Neurooncol* **85**, 281–287.

[56] Kim HP, Yoon YK, Kim JW, Han SW, Hur HS, Park J, Lee JH, Oh DY, Im SA, Bang YJ, et al. (2009). Lapatinib, a dual EGFR and HER2 tyrosine kinase inhibitor, downregulates thymidylate synthase by inhibiting the nuclear translocation of EGFR and HER2. *PLoS One* **4**, e5933.

Table W1. Serial Dilution of GBM CSCs.

	GBM CSCs Injected	Mice with Tumors	Days to Tumor
22 GBM CSC (+)EGF (+)bFGF	100,000	2/2	106
	10,000	2/2	106
	1000	2/2	112-169
	100	3/3	125-188
12.1 GBM CSC (+)EGF (+)bFGF	100,000	2/2	96-109
	10,000	2/2	109
	1000	3/3	109-186
	100	2/3	109-186
22 GBM CSC (–)EGF (–)bFGF	100,000	3/3	90-104
12.1 GBM CSC (–)EGF (–)bFGF	100,000	3/3	83

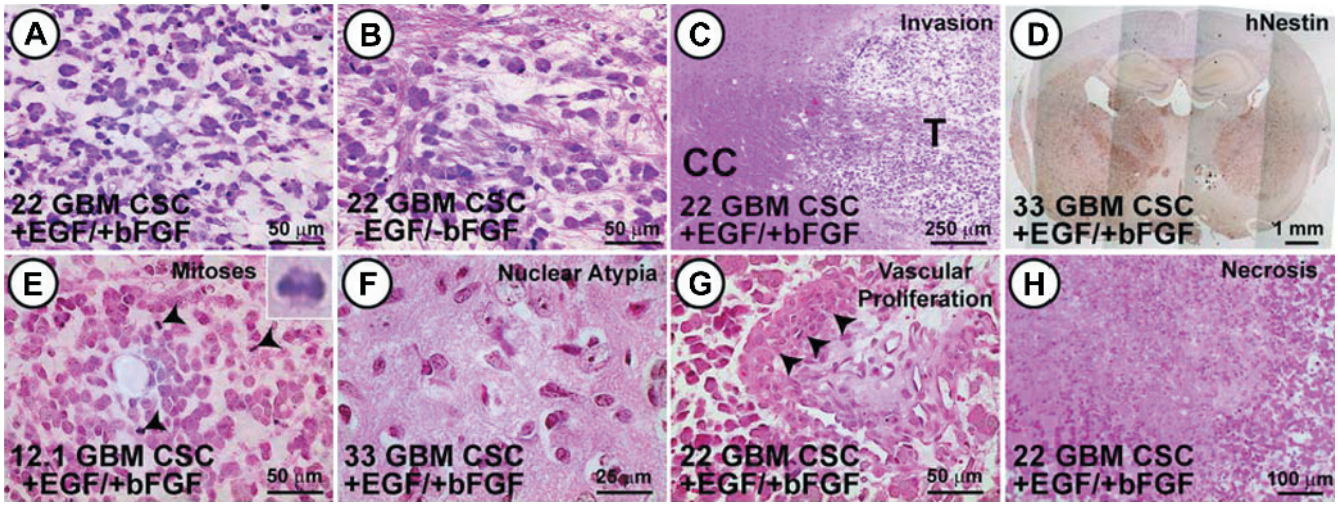

Figure W1. GBM CSCs initiate orthotopic xenografts exhibiting histological hallmarks of human GBM. Although 22 GBM CSCs initiated mostly discrete tumors (A; Figure 1), tumor (T) cell invasion could be identified into the corpus callosum (CC) (C). The 33 GBM CSC line initiated highly diffuse tumors, visualized using a human-specific nestin antibody (hNestin), and tumor cells could be identified in the contralateral brain (D, brown is hNestin^{+} cells). Frequent mitoses (E, arrowheads and inset) and nuclear atypia (F) were frequently seen in all GBM CSC-derived xenografts. In some large GBM CSC–derived tumors, vascular proliferation (G, arrowheads) and areas of necrosis (H) were readily evident (22 GBM CSC line). GBM CSCs cultured long term in medium −EGF/−bFGF did not lose tumor initiation capability (B).

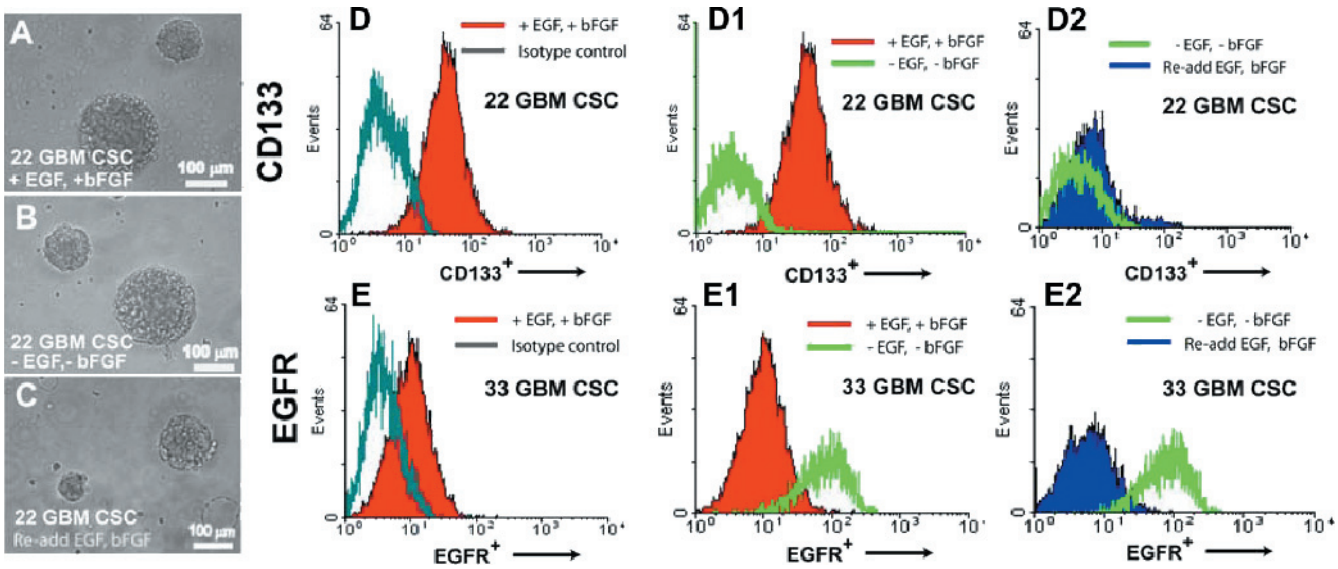

Figure W2. GBM CSCs continued to form spheres and propagate in medium −EGF/−bFGF (B), appearing similar to GBM CSC spheres grown in +EGF/+bFGF medium (A). In medium −EGF/−bFGF, GBM CSCs increased expression of EGFR (E, E1) and CD133 expression was greatly reduced (D, D1), as demonstrated by flow cytometry. Readdition of mitogens and subsequent sphere formation (C) did not increase CD133 expression in GBM CSCs (D2) but reduced EGFR levels (E2).

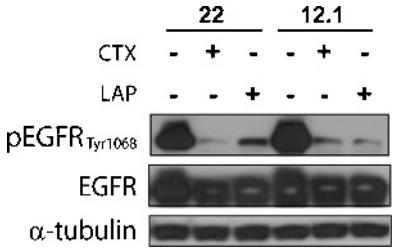

Figure W3. Lapatinib and cetuximab inhibit EGFR activation in GBM CSC lines. After overnight exogenous mitogen removal and addition of lapatinib (LAP, 5 μM) or cetuximab (CTX, 100 nM) for 2 hours, GBM CSCs were stimulated for 30 minutes with EGF (20 ng/ml) before protein collection. Subsequent immunoblot analysis demonstrated robust inhibition of EGFR activation (tyrosine 1068 phosphorylation) by both pharmacologic agents.

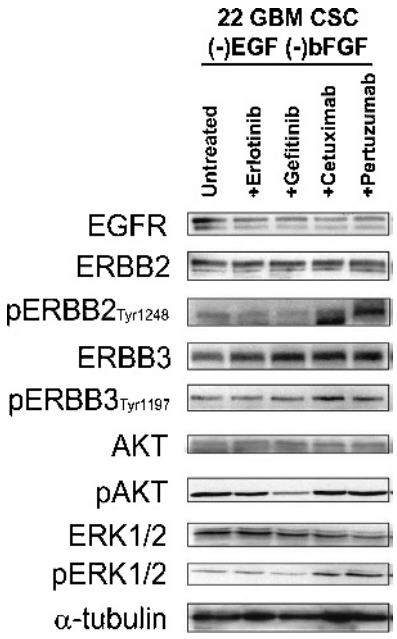

Figure W4. Monospecific EGFR inhibitors do not inhibit downstream effectors of ERBB family signaling. 22 GBM CSCs were incubated overnight with various EGFR-inhibiting agents: erlotinib (1 μM), gefitinib (1 μM), cetuximab (100 nM), or pertuzumab (100 nM). After protein collection, immunoblot analysis was performed to examine ERBB family receptor activation and downstream signaling. Minimal reduction in downstream AKT or ERK1/2 activation was observed for all EGFR inhibitors tested. Treatment with monoclonal blocking antibodies additionally resulted in activation of ERBB family receptors ERBB2 and ERBB3.